Supporting information

Clicked polycyclic aromatic hydrocarbon as a hybridization-responsive fluorescent artificial nucleobase in pyrrolidinyl peptide nucleic acids

Woraluk Mansawat,[a] Chalothorn Boonlua,[a] Khatcharin Siriwong,[b] and Tirayut Vilaivan [a,]*

[a]Organic Synthesis Research Unit, Department of Chemistry, Faculty of Science, Chulalongkorn University, Phayathai Road, Patumwan, Bangkok 10330, Thailand.
[b]Department of Chemistry and Center for Innovation in Chemistry, Faculty of Science, Khon Kaen University, Khon Kaen 40002, Thailand.

*E-mail: vtirayut@chula.ac.th

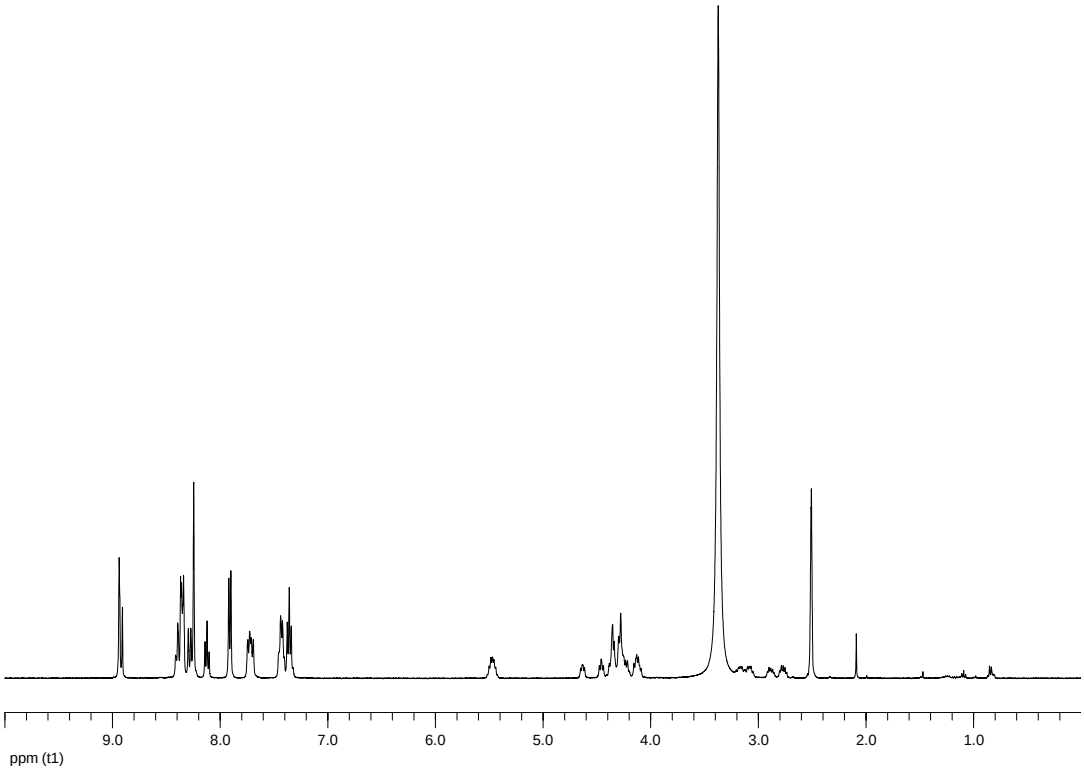

(a)

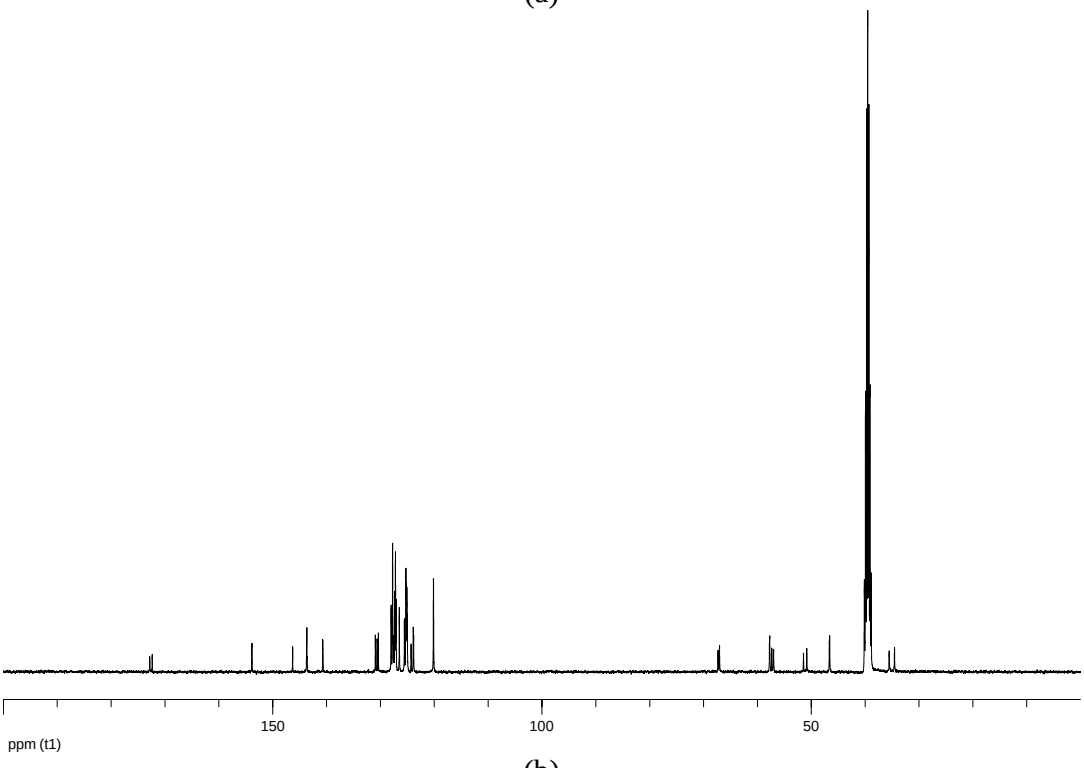

(b)

Fig. S1. ^{1}H (400 MHz, DMSO-d_6) (a) and ^{13}C NMR (100 MHz, DMSO-d_6) (b) spectra of **4**.

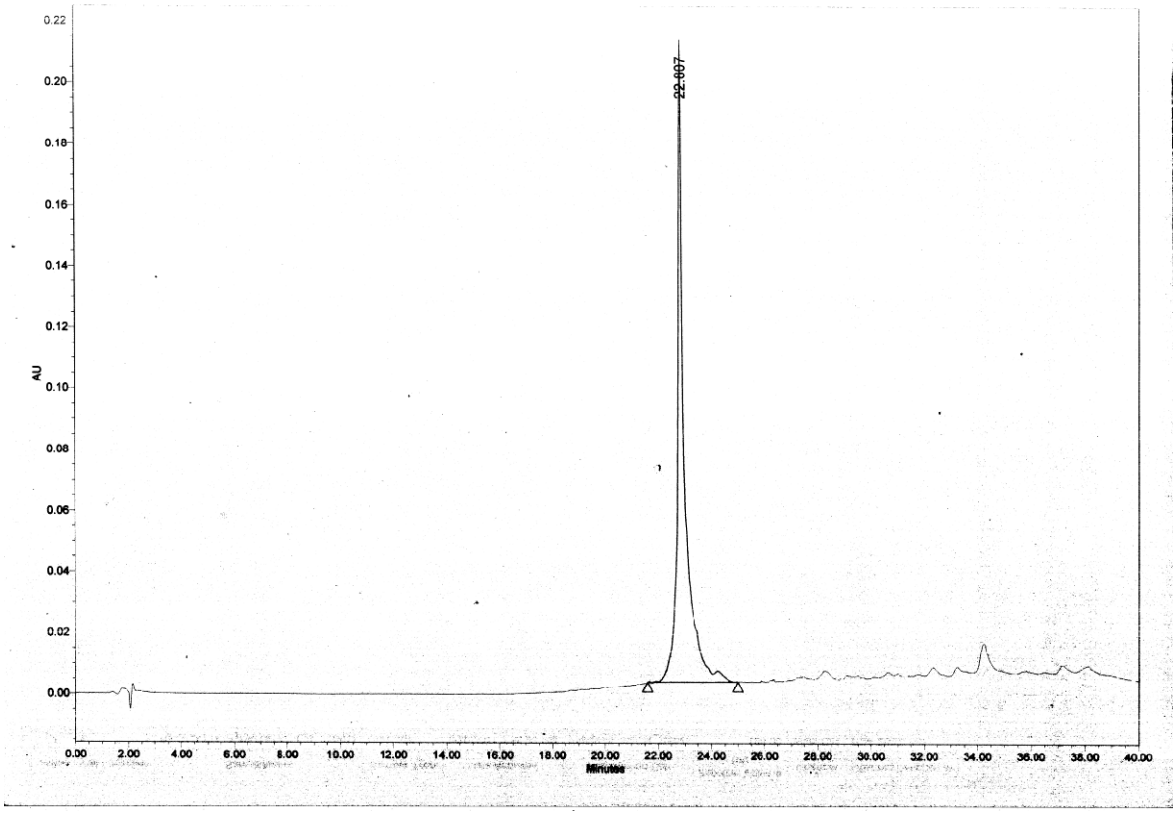

(a)

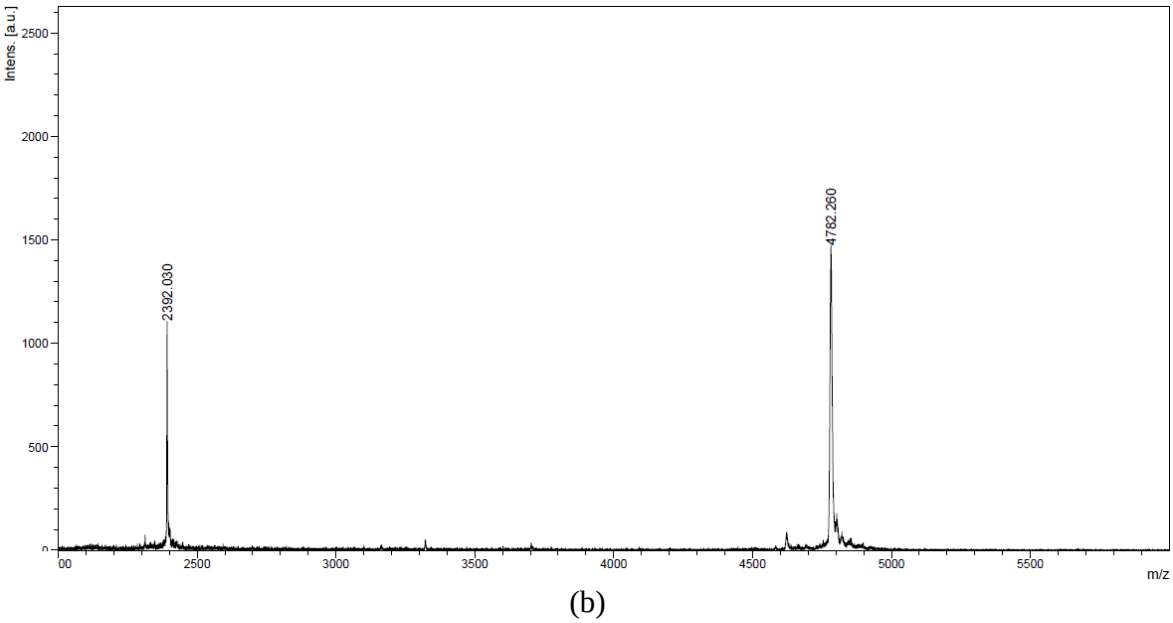

(b)

Fig. S2. Analytical HPLC chromatogram (a) and MALDI-TOF mass spectrum (b) of **PNA1** (Bz-GCATTA**X**AGATAC-LysNH$_2$; **X** = Tz^{Py}) obtained by pre-formed Tz^{Py} monomer (CCA matrix) (calcd. for $[M+H]^+$: *m/z* = 4779.2).

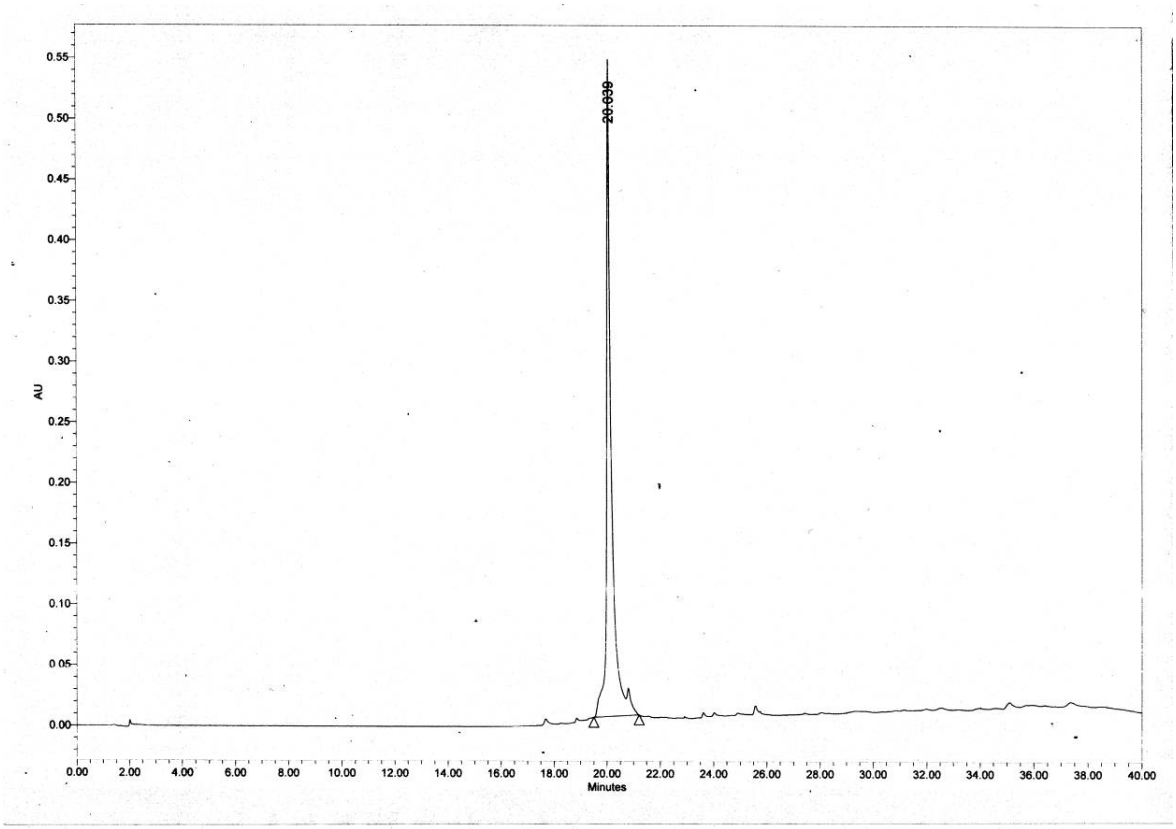

(a)

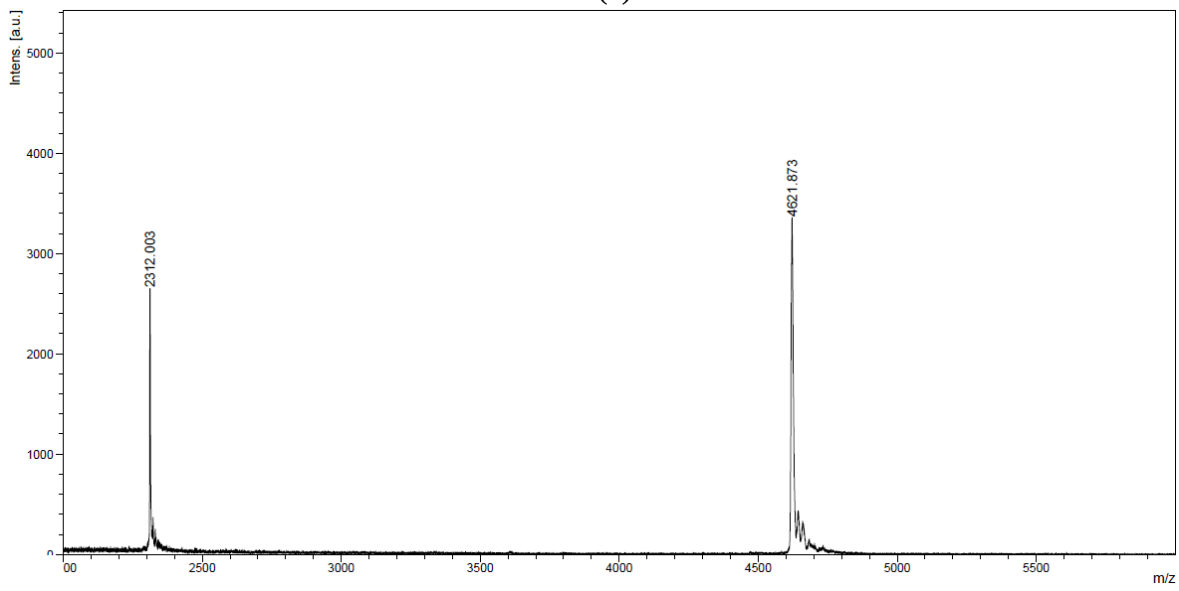

(b)

Fig. S3. Analytical HPLC chromatogram (a) and MALDI-TOF mass spectrum (b) of **PNA2** (Bz-GCATTA**X**AGATAC-LysNH_2; **X** = C) (CCA matrix) (calcd. for $[M+H]^+$: *m/z* = 4621.0).

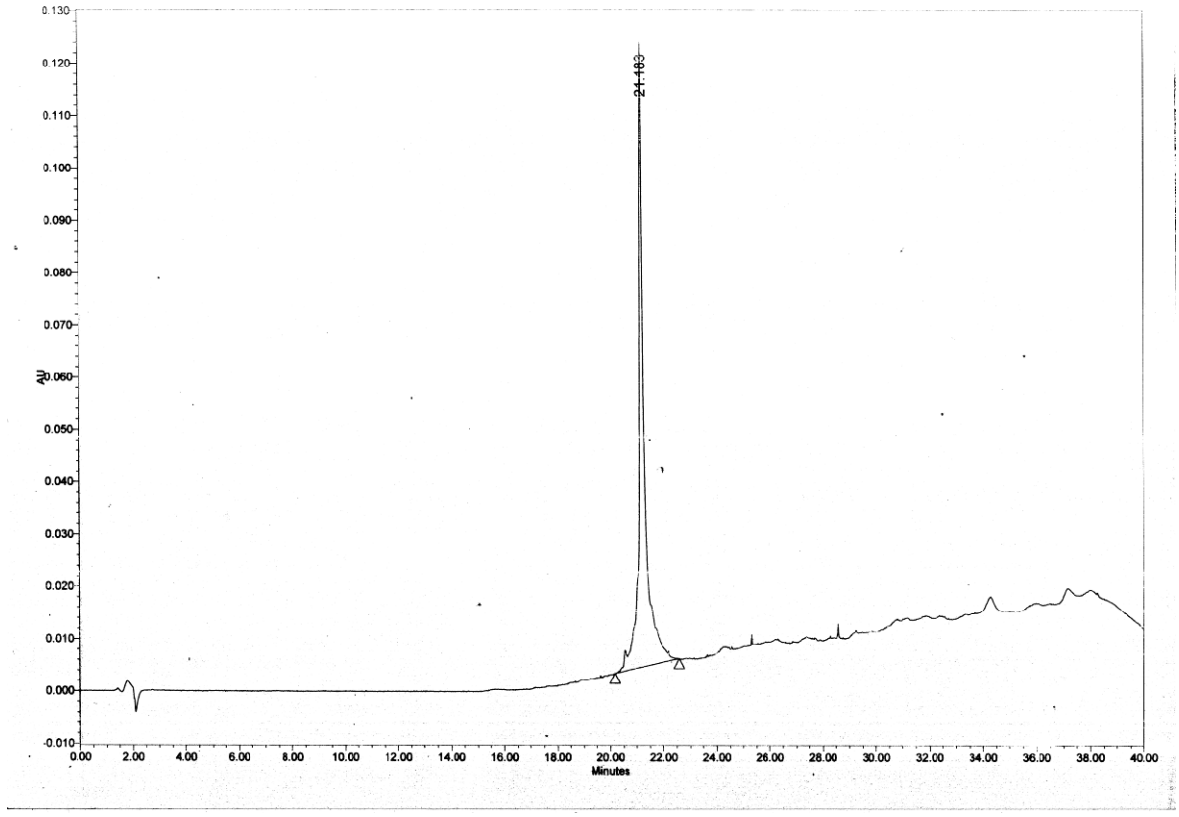

(a)

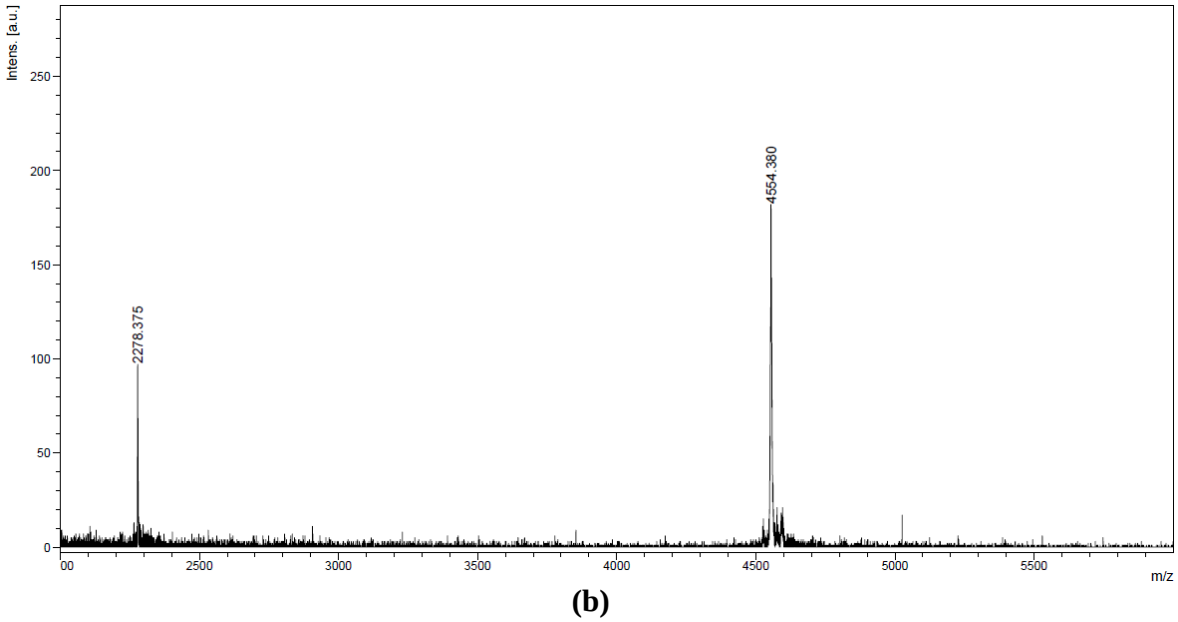

(b)

Fig. S4. Analytical HPLC chromatogram (a) and MALDI-TOF mass spectrum (b) of **PNA3** (Bz-GCATTA**X**AGATAC-LysNH$_2$; **X** = N$_3$) (CCA matrix) (calcd. for $[M+H]^+$: *m/z* = 4552.9).

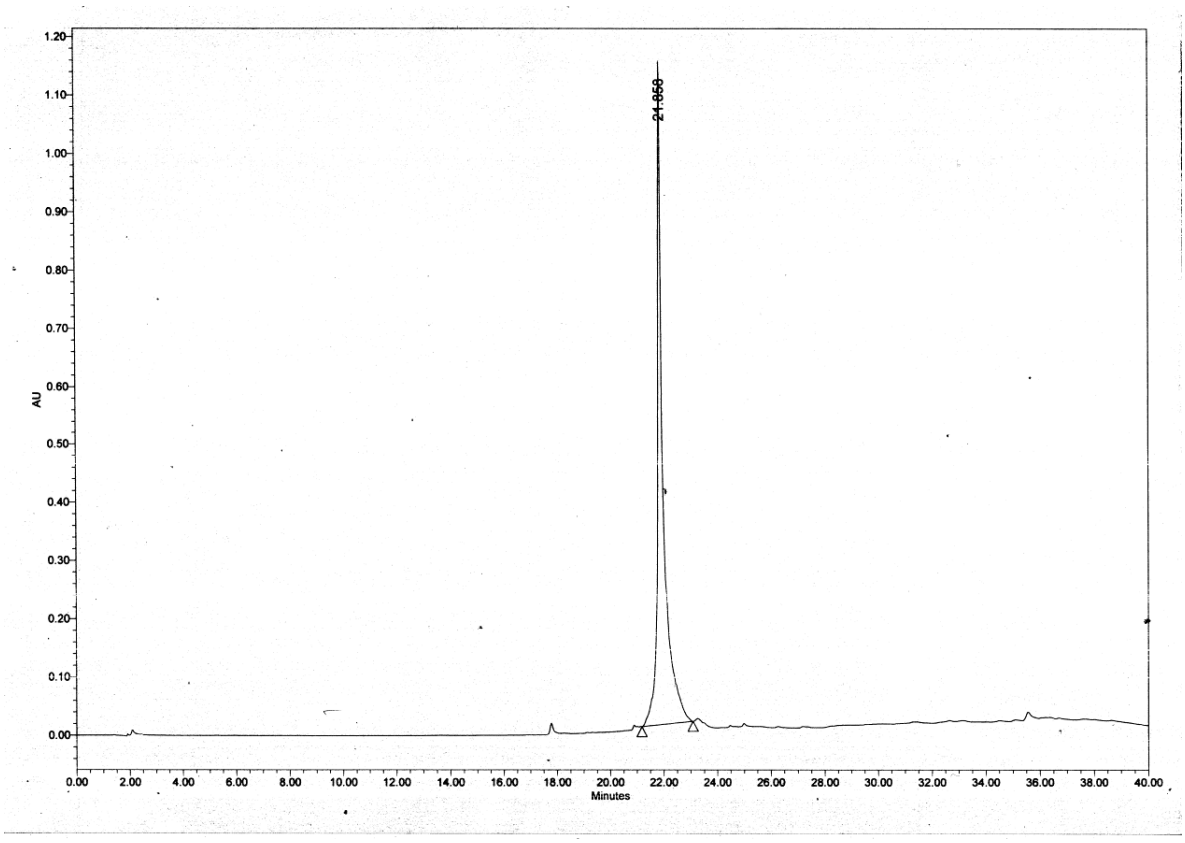

(a)

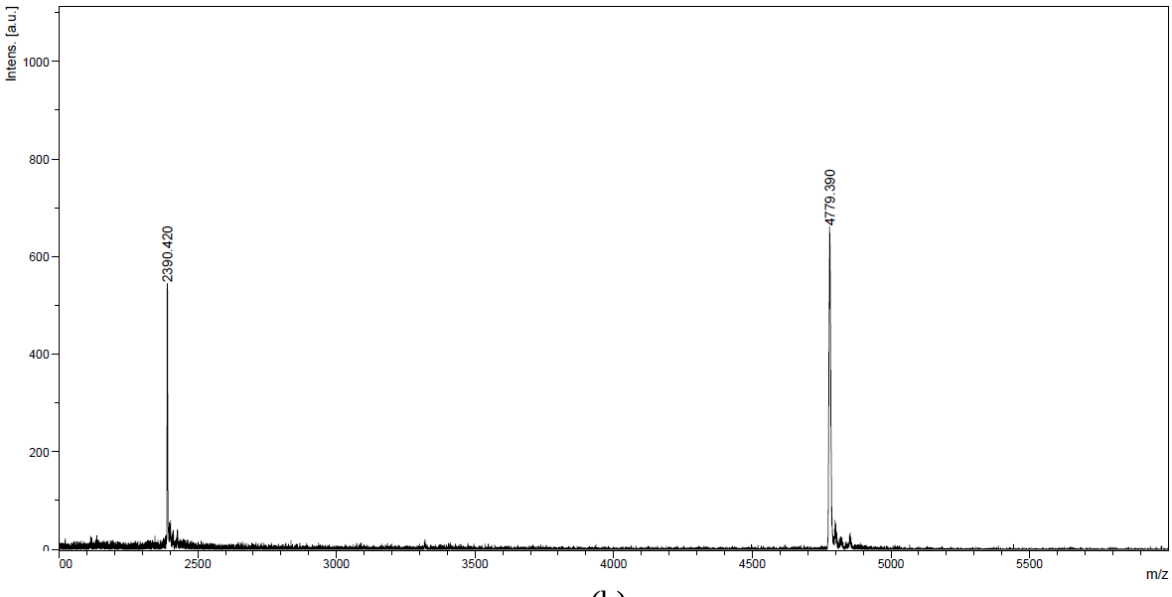

(b)

Fig. S5. Analytical HPLC chromatogram (a) and MALDI-TOF mass spectrum (b) of **PNA1** (Bz-GCATTA**X**AGATAC-LysNH$_2$; **X** = Tz^{Py}) obtained by post-synthetic click reaction (CCA matrix) (calcd. for $[M+H]^+$: *m/z* = 4779.2).

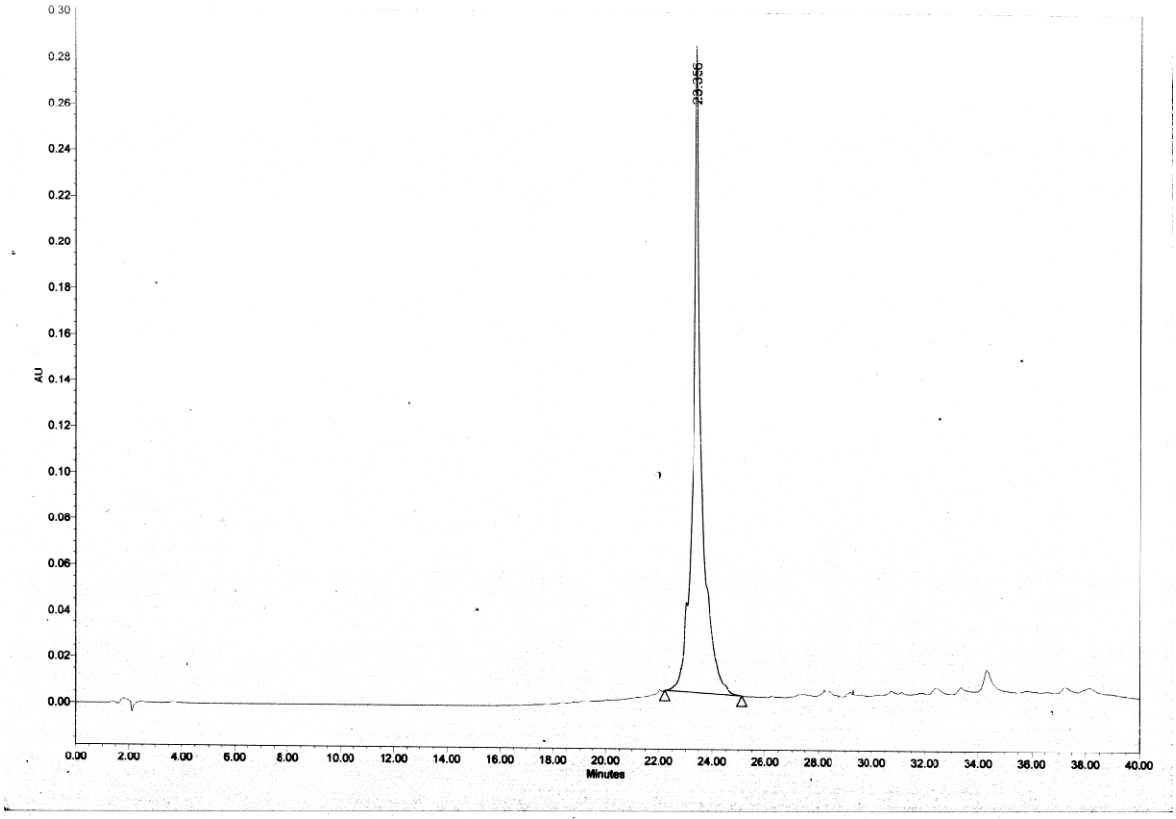

(a)

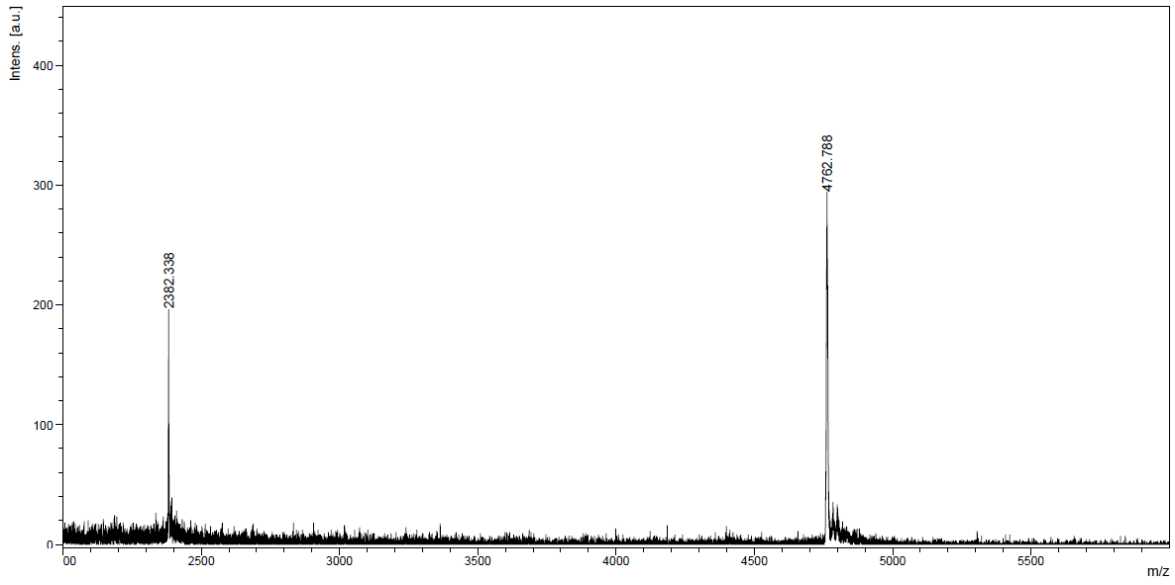

(b)

Fig. S6. Analytical HPLC chromatogram (a) and MALDI-TOF mass spectrum (b) of **PNA5** (Bz-GCATTT**X**TGATAC-LysNH$_2$; **X** = Tz^{Py}) (CCA matrix) (calcd. for $[M+H]^+$: *m/z* = 4761.2).

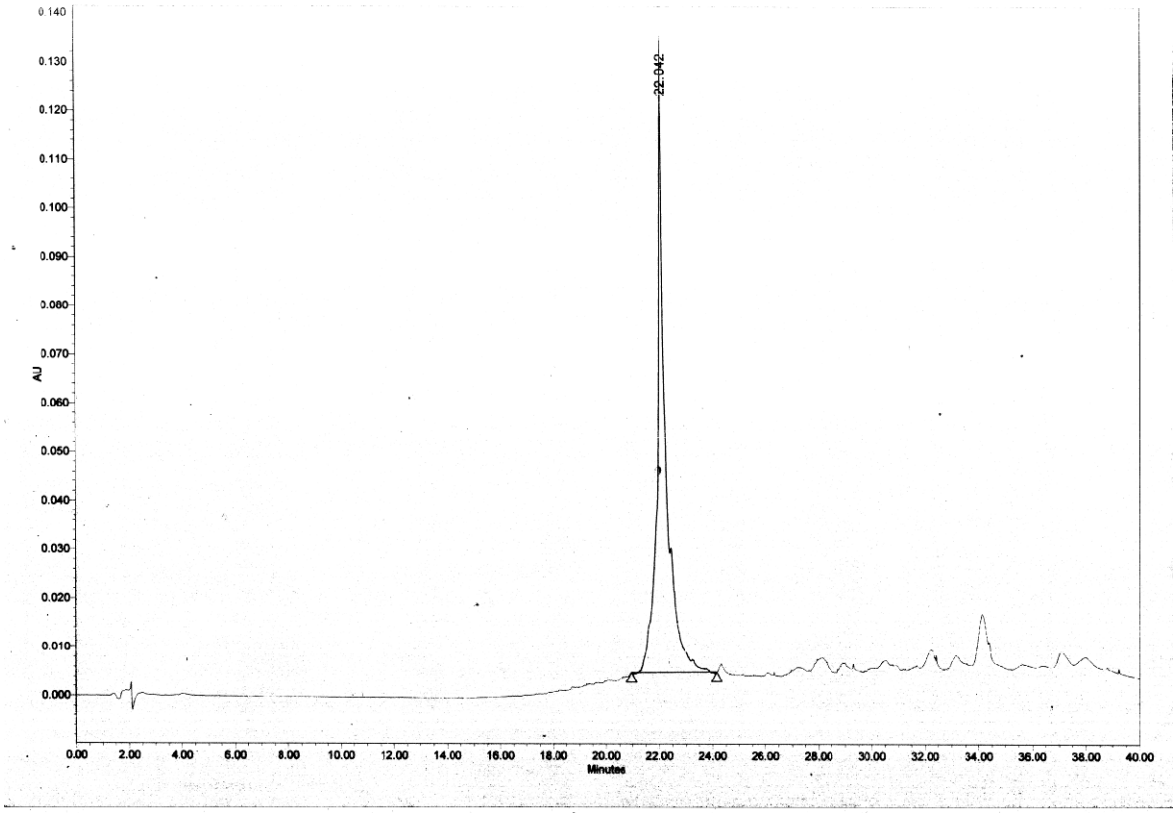

(a)

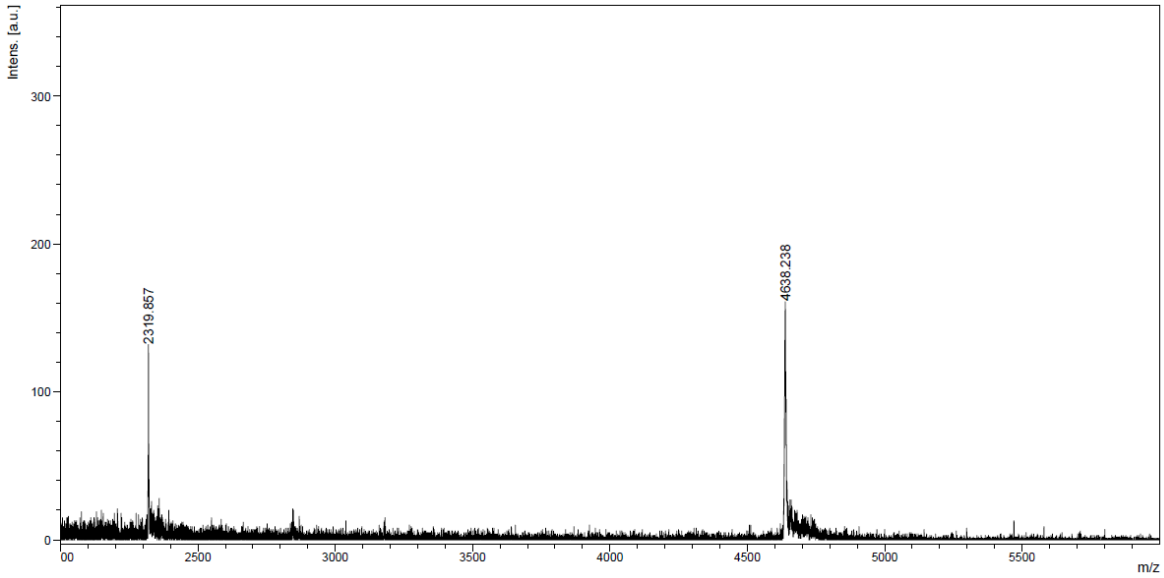

(b)

Fig. S7. Analytical HPLC chromatogram (a) and MALDI-TOF mass spectrum (b) of **PNA6** (Bz-GCATTT**X**TGATAC-LysNH_2; **X** = Tz^{Ph}) (CCA matrix) (calcd. for $[M+H]^+$: m/z = 4637.0).

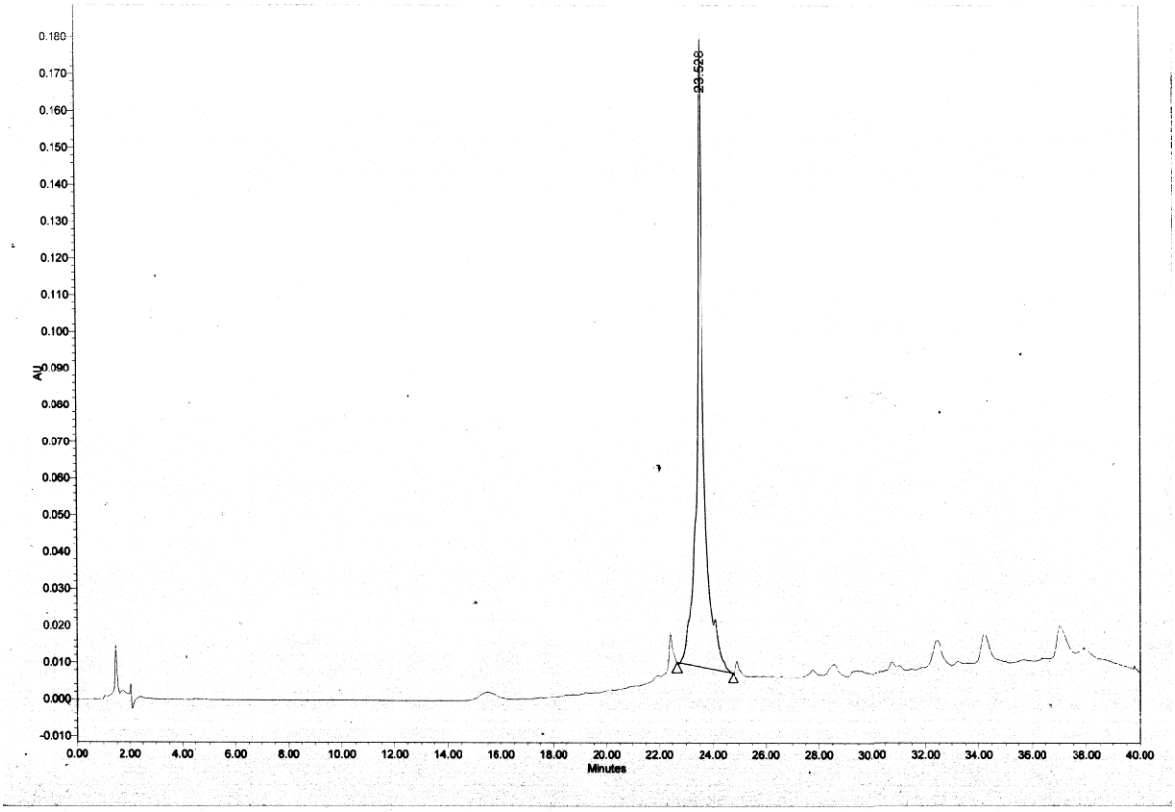

(a)

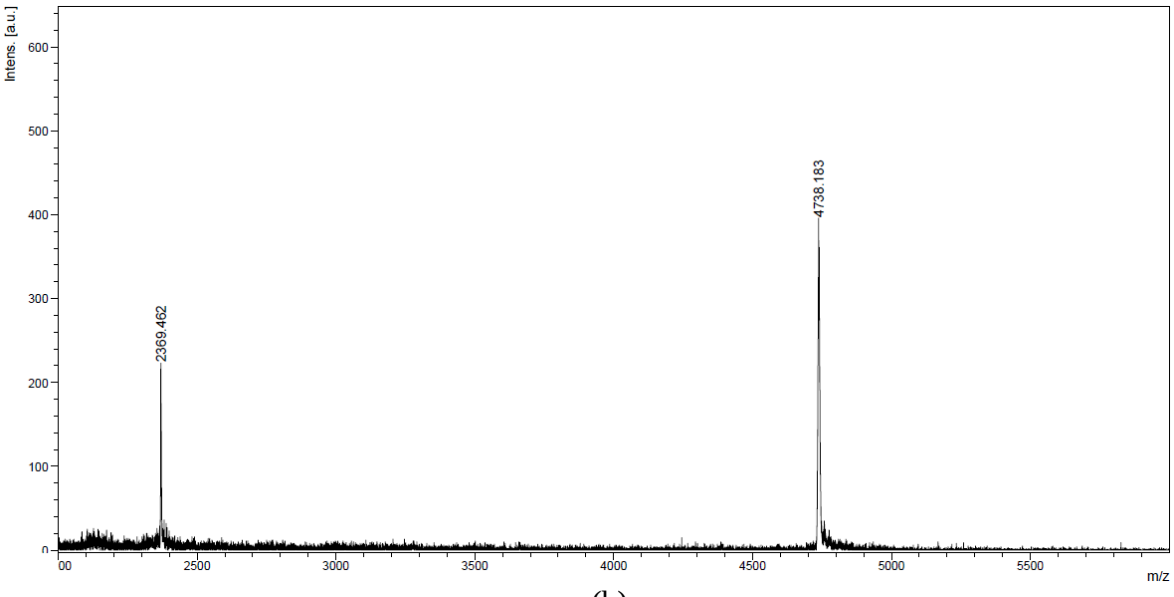

(b)

Fig. S8. Analytical HPLC chromatogram (a) and MALDI-TOF mass spectrum (b) of **PNA7** (Bz-GCATTT**X**TGATAC-LysNH_2; **X** = Tz^{An}) (CCA matrix) (calcd. for $[M+H]^+$: *m/z* = 4737.1).

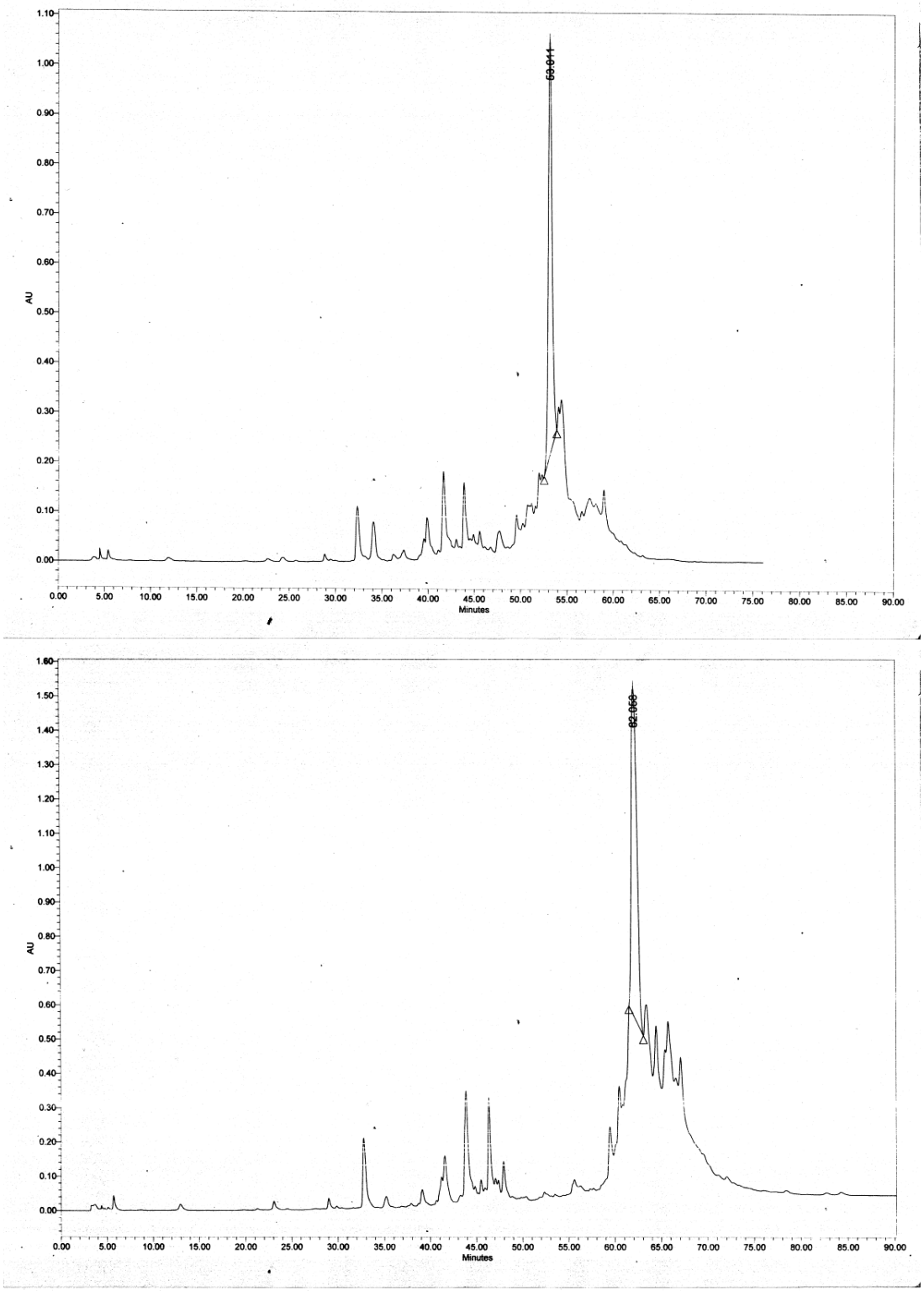

Fig. S9. HPLC chromatogram of crude **PNA3** (Bz-GCATTA**N$_3$**AGATAC-LysNH$_2$) before (top) and after (bottom) click reaction with 1-ethynylpyrene.

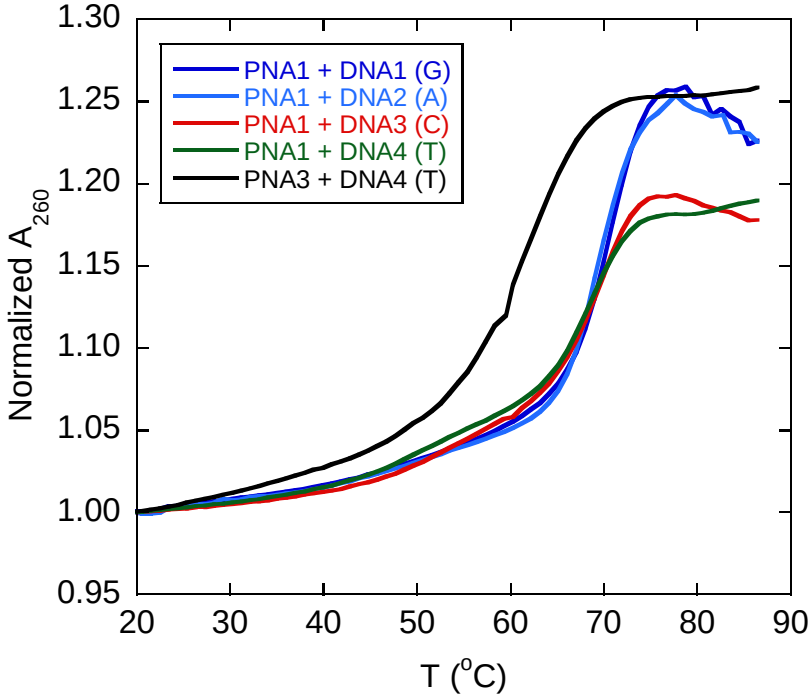

Fig. S10. Thermal denaturation curves of hybrids between **PNA1** (Tz^{Py}) with **DNA1–DNA4** and **PNA3** (azide) with **DNA4**. Conditions: 2.5 µM PNA, 3.0 µM DNA in 10 mM sodium phosphate buffer pH 7.0.

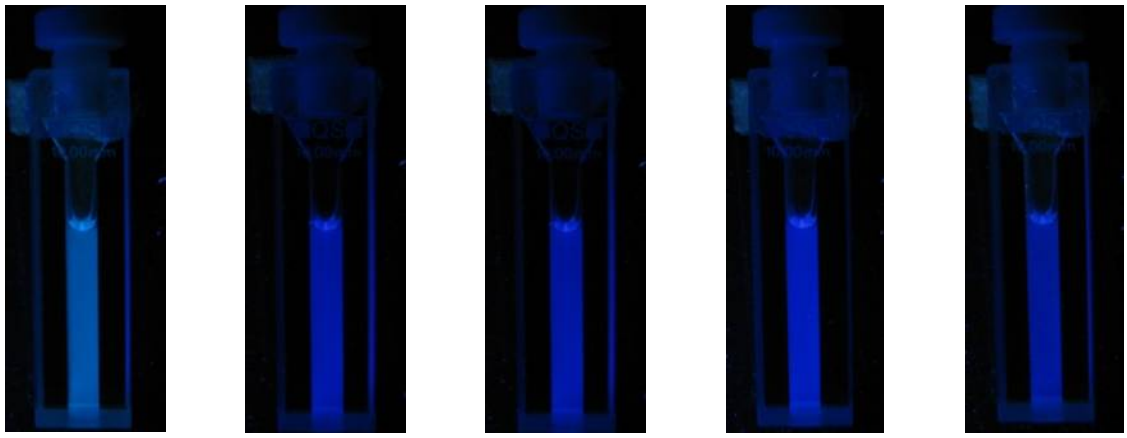

PNA1 ss | **+DNA1** Y = G | **+DNA2** Y = A | **+DNA3** Y = C | **+DNA4** Y = T

Fig. S11. Photographs of **PNA1** and its hybrids with **DNA1**–**DNA4** viewed under black light. Conditions: 2.5 μM PNA, 3.0 μM DNA in 10 mM sodium phosphate buffer pH 7.0.

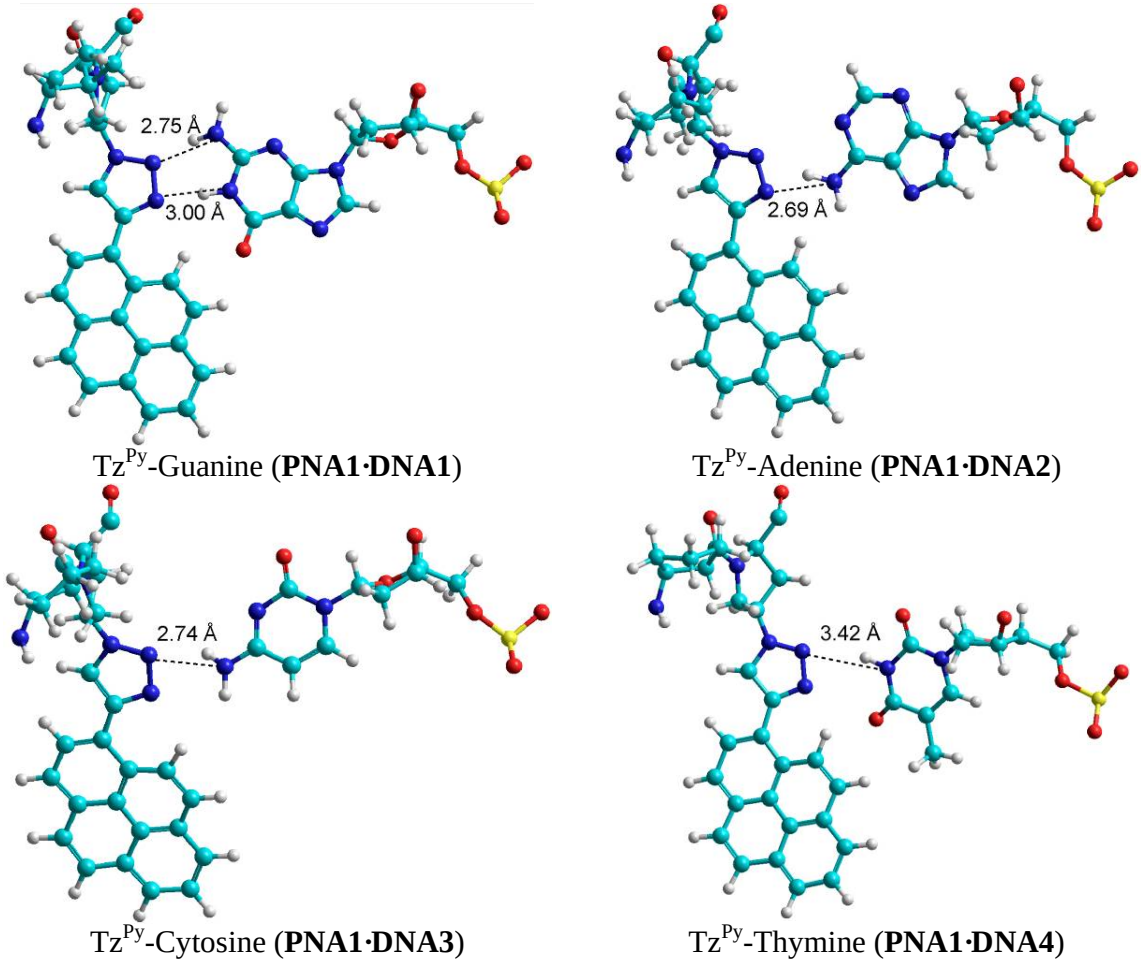

Tz^{Py}-Guanine (**PNA1·DNA1**) Tz^{Py}-Adenine (**PNA1·DNA2**)

Tz^{Py}-Cytosine (**PNA1·DNA3**) Tz^{Py}-Thymine (**PNA1·DNA4**)

Fig. S12. Selected snapshots of MD structures showing the hydrogen-bond formation between Tz^{Py} and opposite base for four simulated systems. The hydrogen bond acceptor-donor distances are shown.

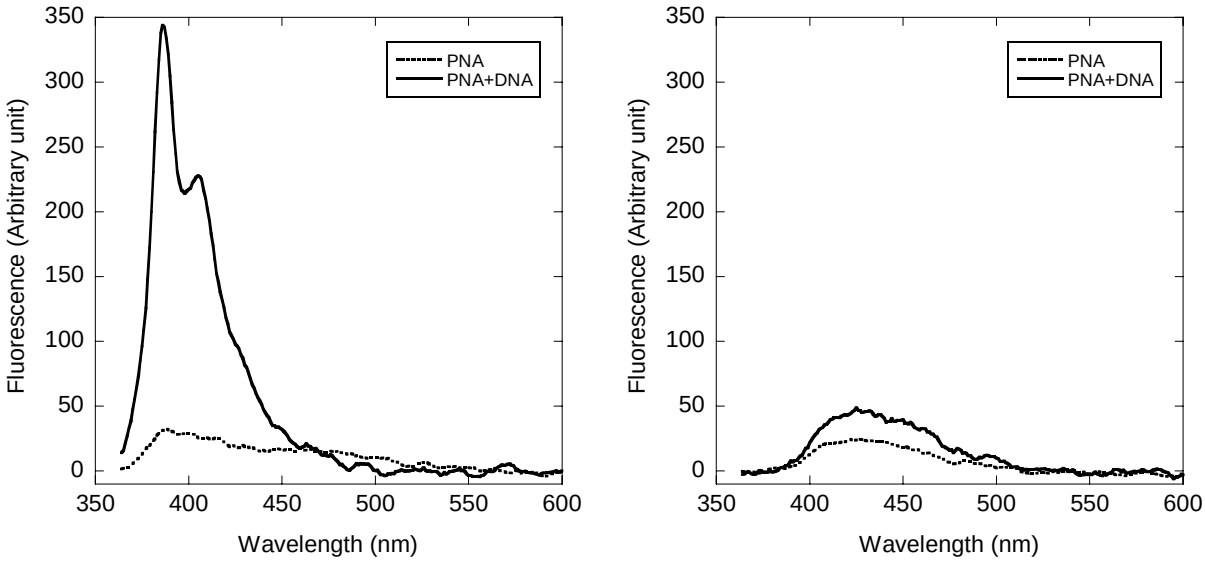

Fig. S13. Fluorescence spectra of **PNA5** (a) and **PNA7** (b) in the absence (···) and presence (–) of complementary DNA (5'-GTATCAGAAATGC-3') (conditions: 2.5 µM PNA, 3.0 µM DNA in 10 mM sodium phosphate buffer pH=7.0, λ_{excit} = 350 nm).